Scattered-wave study of the magnetic properties of the potassium trimer

E. R. Dietz*
Department of Physics, University of California, Berkeley, California 94720
(Received 17 July 1980)

The $X\alpha$ scattered-wave (XASW) technique is applied to the trimer of potassium, and the appearance of the high-field electron-spin-resonance (ESR) spectrum is predicted. Contact spin densities, including core-polarization contributions, are calculated for several different structures; the resulting model hyperfine patterns strongly reflect the assumed geometrical configuration of the atoms. Comparison of these model spectra with experimental results is discussed.

I. INTRODUCTION

Within the past two decades there has been a rapidly growing interest among physicists and physical chemists in the structure and properties of small metallic aggregates. Experimental and theoretical studies of the electronic properties of such aggregates has been stimulated in part by their potential for technological application, for example in catalysis.[1] More fundamentally, the evolution with size of the equilibrium-geometrical configuration, the nature of the bonding, and the cohesive energies along with the magnetic, thermal, and optical properties are topics of current interest.

Aggregates of Na and K containing three and five atoms have been identified in electron-spin-resonance (ESR) experiments performed by Lindsay *et al.*[2,3] on alkali metal deposited in a frozen inert-gas matrix. Structural information deduced from experiments of this sort, however, may reflect the characteristics of the matrix trapping site rather than the equilibrium-geometrical configuration of the naked aggregate. Small alkali aggregates containing from 2 to 16 atoms have been studied using molecular-beam techniques[4-10] which have yielded photoionization thresholds for the free species Na_x and K_x as well as optical excitation spectra for Na_2, K_2, and Na_3. In our laboratory, a molecular-beam magnetic-resonance (MBMR) experiment[11,12] designed to yield structural information with regard to the smallest paramagnetic alkali aggregates (i.e., those containing odd numbers of valence electrons) is currently in progress.

As detailed in Table I, much calculational effort has been invested in the determination of stabilities and electronic structures for the alkali trimer aggregates.[13-27] Among the best calculations for the whole-molecule properties, e.g., stability, are those which employ the *ab initio* restricted Hartree-Fock (RHF) technique with configuration interaction (CI). For properties which depend heavily on accurate one-electron wave functions and eigenvalues (e.g., ionization potentials and spin densities), however, the $X\alpha$ scattered-wave technique (XASW) of Slater and Johnson provides, cost effectively, results which are competitive with those from the *ab initio* calculations. We describe here the results of XASW calculations on K_3 which may be compared with ESR measurements to obtain structural information regarding this species. In Sec. II we present some details of the calculations; Sec. III contains results for the total spin densities at the K_3 nuclei along with predictions of the high-field ESR patterns.

II. THE COMPUTATION

Both the conceptual basis[28] and the practical techniques[29] for the implementation of the XASW method are extremely well documented elsewhere, so that we need only briefly describe the salient features of the method. The starting point of the theory is the $X\alpha$ statistical total energy

$$\langle E_{X\alpha}\rangle = \sum_i n_i \int u_i^*(1) f_1 u_i(1)\, dv_1 + \tfrac{1}{2}\int \rho(1)\rho(2) g_{12}\, dv_1 dv_2 + \tfrac{1}{2}\int [\rho_\uparrow(1) U_{X\alpha\uparrow}(1) + \rho_\downarrow(1) U_{X\alpha\downarrow}(1)]\, dv_1 . \quad (1)$$

In this expression $u_i(\vec{r})$ is the wave function for the spin orbital i, f_i is the (kinetic + nuclear potential) one-electron operator acting on orbital i, g_{12} is the two-electron Coulomb operator, and $\rho(\vec{r})$ is the local electronic charge density

$$\rho = \rho_\uparrow + \rho_\downarrow ,$$
$$\rho_\uparrow = \sum_{j\uparrow} n_j i_{j\uparrow} u_{j\uparrow}^* , \quad \rho_\downarrow = \sum_j n_j u_{j\downarrow} u_{j\downarrow}^* . \quad (2)$$

The arrow subscripts indicate relative spin orientations. For the final term in Eq. (1) we use Slater's approximation to the exchange potential

$$U_{X\alpha\uparrow} = -9\alpha[(3/4\pi)\rho_\uparrow]^{1/3} , \quad (3)$$

with a similar expression for $U_{X\alpha\downarrow}$ to obtain, by variation of $\langle E_{X\alpha}\rangle$, the one-electron equation for

 © 1981 The American Physical Society

TABLE I. Recent calculations on alkali-metal trimers.[a]

Year (Ref.)	Aggregate	Method	Geometry	Angle[b]	State	Stability (eV)[c] $M_3 \rightarrow M + M_2$
1968 (13)	Li_3	DIM[d]	C_{2v}	137°	$^2A_1$	0.4
1969 (14)	Li_3	DIM	C_{2v}	136°	$^2B_2$	0.4
1973 (16)	Li_3, Na_3	DIM	$D_{\infty h}$	180°	$^2\Sigma_u^+$	0.3, 0.1
1975 (17)	Na_3	DIM	C_{2v}	46°	$^2A_1$	0.2
1975 (18)	Li_3	SCF-$X\alpha$[e]	(D_{3h})	(60°)	$(^2A'')$	0.2
1975 (19)	Na_3	CNDO[f]	C_{2v}			unstable
1975 (19)	Na_3	EH[g]	$D_{\infty h}$	180°	$^2\Sigma_u^+$	0.6
1972 (15)	Na_3, K_3	PP[h]	$D_{\infty h}$	180°	$^2\Sigma_u^+$	unstable
1976 (21)	Li_3	RHF[i]	C_{2v}	50°	$^2A_1$	~0.4
1975 (20)	Li_3, Na_3, K_3, Rb_3, Cs_3	PP	$(D_{\infty h})$	(180°)	$(^2\Sigma_u^+)$	
1978 (24)	Na_3	CI[j]	C_{2v}	73°	$^2B_2$	0.4
1978 (25)	Li_3	CEPA[k]	"D_{3h}"	60°	"$^2E'$"	0.4
1978 (26)	Li_3	DIM	C_{2v}	101°	$^2B_2$	0.4
1978 (27)	Li_3	CI	C_{2v}	spin-density calculation		
1977 (22)	Li_3	RHF	C_{2v}		$^2A_2$	spin-population calculation
1977 (23)	Li_3	CI	C_{2v}	70°	$^2B_2$	0.4 (equally stable)
				50°	$^2A_1$	

[a] Compiled in part by Lindsay *et al.* (Ref. 2).
[b] Indicates bond angle included at nonequivalent atom for the configuration with lowest energy of those considered in the calculation.
[c] Quoted with respect to dissociation to atom + dimer. Parentheses indicate assumed structure. Quotation marks indicate effective or time-average fluctuational geometry.
[d] DIM, diatomics in molecules.
[e] SCF-$X\alpha$, self-consistent-field $X\alpha$ calculation.
[f] CNDO, complete neglect of differential overlap.
[g] EH, extended Huckel.
[h] PP, pseudopotential.
[i] RHF, restricted Hartree-Fock.
[j] CI, configuration interaction.
[k] CEPA, coupled electron pair approximation.

the spin-orbitals $u_{i\uparrow}$ (in atomic units):

$$\{-\nabla_i^2 + V_c(1) - 6\alpha[(3/4\pi)\rho_\uparrow]^{1/3}\} u_{i\uparrow}(1) = \epsilon_i u_{i\uparrow}(1) . \quad (4)$$

The parameter α is introduced in Eq. (3) to improve this approximation to the exchange interaction for different materials. We have taken for potassium $\alpha_K = 0.721\,17$ in accordance with the table of values compiled by Schwartz[30] based on the Hartree-Fock total energies of Mann.[31] To solve Eq. (4) for the spin orbitals of the aggregate, space is partitioned as in Fig. 1. The one-electron Coulomb potential $V_c(1)$ is converted to an approximate muffin-tin form by spherically averaging V_c in regions I and III, while for region II a constant potential equal to the volume average over this region is assumed. The sphere radii are chosen so that a fair amount of overlap is introduced to reduce the size of the region in which V_c is approximated by a constant, in accordance with a procedure suggested by Salahub *et al.*[32] Equation (4) is now solved in each region with the muffin tin V_c using the Numerov method[33] to determine the radial part of the wave function in regions I and III. A scattered-wave formalism is then used to impose continuity of the wave function and its first derivative across the muffin-tin boundaries.

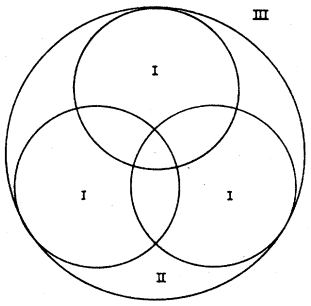

FIG. 1. Partitioning of space for an XASW calculation on trimers. In regions I, the atom spheres, the potential is spherically averaged, as it is in the extramolecular region III. In region II a simple volume average of the potential is used. The overlap of regions I reduces the volume of the region in which the volume average must be used; the extent of the overlap is determined by the Salahub-Roberge procedure described in the text.

The spin orbitals obtained in this way determine a new charge density and potential to be used in the next iteration. The procedure is repeated until a preset level of self-consistency is attained.

Our experience with preliminary calculations on K_2 confirms observations made by other workers regarding the inaccuracies introduced by use of the muffin-tin approximation in the determination of whole-molecule properties such as stability. The calculated binding energy ϵ_B for K_2 was seen to vary from 0.16 to 0.96 eV as the muffin-tin spheres went from contiguity to 30% overlap; these values are to be compared with the experimental dissociation energy[34] of 0.51 eV. The ionization potential of K_2, in contrast, is within 0.1 eV of the measured threshold.[7] This is consistent with our expectation that the XASW approach is most appropriate to one- or few-electron properties, in particular those which depend on the behavior of the orbital wave functions near the nucleus (e.g., hyperfine and spin-orbit interactions), where the muffin-tin approximation is believed to be a fairly good one.

A preliminary set of spin-restricted calculations were performed on K_3 with the geometries and sphere radii listed as set I of Table II. The coordinates (Q_a, Q_y, Q_x) listed in the first column re-

TABLE II. Geometrical parameters for XASW calculations on K_3.

Set I [a] (Q_a, Q_y, Q_x) [b] (a.u.)	$R_{12}=R_{13}$ [c] (a.u.)	R_{23} [c] (a.u.)	θ_A [d] (deg)	RS(0) [e] (a.u.)	RS(1,2,3) [e] (a.u)
(0,0,0)	8.60	8.60	60	10.56	5.59
(0.5,0.0)	9.10	9.10	60	11.17	5.92
(−0.5,0,0)	8.10	8.10	60	9.94	5.26
(0.25,0,0)	8.85	8.85	60	10.86	5.75
(−0.25,0,0)	8.35	8.35	60	10.25	5.43
(0,0.31,0)	8.48	8.85	63	10.48	5.51
(0,0.61,0)	8.35	9.10	66	10.41	5.43
(0,1.22,0)	8.10	9.60	73	10.29	5.26
(0,1.84,0)	7.85	10.10	80	10.23	5.10
(0,2.45,0)	7.60	10.60	88	10.24	4.94

Set II [a] θ_A (deg)	$R_{12}=R_{13}$ (a.u.)	R_{23} (a.u.)	RS(0) (a.u.)	RS(1,2,3) (a.u.)
180	8.60	17.26	14.19	5.59
90	8.60	12.16	11.67	5.59
75	8.60	10.47	11.01	5.59
60	8.60	8.60	10.56	5.59
55	8.60	7.94	10.01	5.16
50	8.60	7.27	9.47	4.72

[a] Set I pertains to the energy hypersurface calculations plotted in Fig. 2. Set II pertains to the spin-density calculations.

[b] Normal mode displacements defined in Eq. (5) as functions of the bond-length increments r_{ij}. The $Q_a=Q_y=Q_x=0$ structure is defined as the equilateral configuration with a bond length of $R_{eq}=8.60$ a.u.

[c] The R_{ij} represent the bond lengths in a.u. for each structure, with $i=1$ denoting the apex (nonequivalent) atom.

[d] Included angle at the apex.

[e] The RS(n) represent the muffin-tin sphere radii, with $n=0$ denoting the outer sphere.

present the normal mode distortions

$$Q_a = \tfrac{1}{3}(r_{12}+r_{23}+r_{13}),$$
$$Q_y = \frac{1}{\sqrt{6}}(2r_{23}-r_{13}-r_{12}), \quad (5)$$
$$Q_x = \frac{1}{\sqrt{2}}(r_{13}-r_{12}),$$

from the equilateral configurations with bond length R^o_{eq}. The r_{ij} represents the increments in the distances between atoms i and j, with atom 1 designated as the apex of the triangle. The results for the relative total energies are shown plotted in Fig. 2. The total energy curve for equilateral K_3 in Fig. 2(a) exhibits a minimum at $R^o_{eq} = 8.6$ a.u., which we take as the equilibrium spacing. This value for R^o_{eq} is quite close to an estimate obtained by linear scaling using the known bond lengths[34] for K_2 ($R^o_{eq} = 7.4$ a.u.) and Na_2 ($R^o_{eq} = 5.8$ a.u.) along with Martin and Davidson's theoretical value[24] of R^o_{eq} for Na_3. The behavior of the total energy as shown in Fig. 2(a) was calculated by uniform co-expansion of both the bond lengths and muffin-tin spheres, so that the percentage overlap of the spheres remains constant for the different configurations. Figure 2(b) shows an attempt to locate a Jahn-Teller minimum in total energy resulting from a symmetry-breaking Q_y distortion. No such minimum was found for the $Q_y > 0$ case, in which the distortions could not be represented as uniform co-expansions in contrast with the calculations of Fig. 2(a). The absence of such a minimum is believed to reflect the inaccuracies associated with the muffin-tin approximation.

While it is clear from Table I that some workers have found critical points in the behavior of the total energy for $Q_y < 0$ and $Q_y > 0$, our experience indicates that our muffin-tin approximation will dominate the behavior of the curve for acute[35] distortions as well as for the obtuse configurations discussed above.

III. PREDICTED HYPERFINE STRUCTURE FOR K_3

For a multinuclear system we write the magnetic Hamiltonian, for an external Zeeman field $\vec{H}_0$, as[7]

$$\mathcal{H}_S = -g\mu_0 \vec{S}\cdot\vec{H}_0 - \sum_i \frac{\mu_i}{I_i}\vec{I}_i\cdot\vec{H}_0 + \sum_i\sum_\alpha a_{\alpha i}\vec{S}_\alpha\cdot\vec{I}_i + \mathcal{H}_{anis}. \quad (6)$$

where $\sum_\alpha$ represents a sum over electronic-spin orbitals in the contact hyperfine coupling term, and $\sum_i$ is a sum over nuclei. We consider here only the case $\mu_i = \mu_{39}$, $I_i = I_{39} = \frac{3}{2}$, since 80% of the trimers formed from potassium bulk will be totally $^{39}K_3$. The term $\mathcal{H}_{anis}$ is the anisotropic hyperfine coupling due to the non-s contributions to the electronic wave functions; this term is small and contributes only to the widths, not to the mean positions of the lines. The $a_{\alpha i}$ are the electron-nuclear contact-coupling constants

$$a_{\alpha i} = -\frac{16\pi}{3}\frac{\mu_0\mu_i}{I_i}|\psi_\alpha(\vec{r}_i = 0)|^2 n_\alpha, \quad (7)$$

where n_α is the occupation of spin orbital α. If we define the quantities ξ_i:

$$\xi_i = 2\sum_\alpha |\psi_\alpha(\vec{r}_i = 0)|^2 m_{s\alpha} n_\alpha \left(\sum_\alpha m_{s\alpha} > 0\right), \quad (8)$$

we can rewrite $\mathcal{H}_S$ in the high-field (Paschen-Bach) limit, where m_s and m_I are good quantum numbers, as

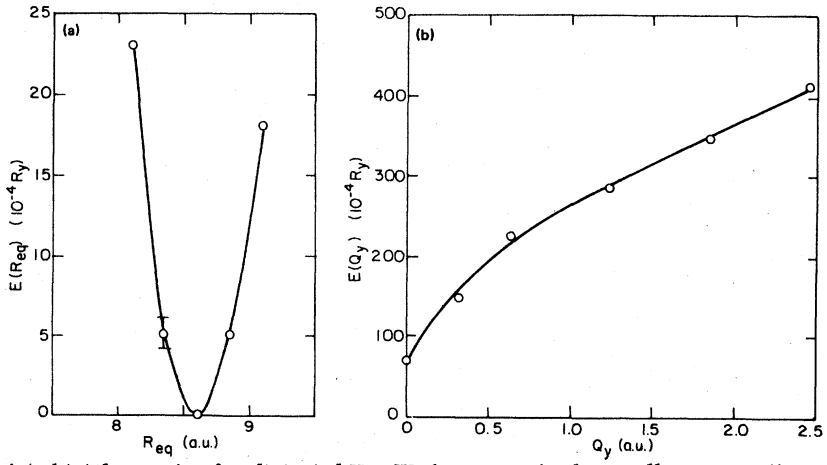

FIG. 2. Spin-restricted total energies for distorted K_3. We have examined a small cross section of the energy hypersurface of K_3 using the XASW routine. In (A) we examine the energy about the Q_a minimum (with $Q_x = Q_y = 0$); (B) shows the result of a distortion in Q_y (with $Q_a = Q_x = 0$). These modes are defined in Eq. (5).

$$\mathcal{H}_S = -g\mu_0 m_s H_0 - \sum_i \frac{\mu_i}{I_i} m_{Ii} H_0 + \frac{8\pi}{3} \frac{\mu_0 \mu_{39}}{I_{39}} \sum_i m_{Ii} \xi_i + \mathcal{H}_{\text{anis}} . \quad (9)$$

The mean resonant fields H_R for the electronic-spin transitions in which $|\Delta m_S| = 1$ are given by

$$H_R = -\frac{\hbar\omega_0}{g\mu_0} + \frac{16\pi}{3g} \frac{\mu_{39}}{I_{39}} \sum_i m_{Ii} \xi_i = H_R^f - H_{\text{loc}} . \quad (10)$$

Here H_R^f is, for an rf transition field of angular frequency ω_0, the resonant field for a free-electron-spin transition; H_{loc} is the effective local field seen by the odd electron as a function of nuclear orientation. We have neglected in expression (10) both the shift in the free-electron gyromagnetic ratio and the second-order shift in the resonance field due to the electron-nuclear coupling, which vanishes for sufficiently large H_0. The positions of the spin resonances in the high-field limit depend on the parameters ξ_i which we have calculated, using the XASW wave functions, for several different configurations of K_3 in which the distance between the apex and base atoms is kept at $R_{\text{eq}}^o = 8.6$ a.u., while the apex angle θ_A is varied. The geometrical parameters for these calculations are given in Table II under set II; the spin-unrestricted results for the ξ_i are displayed in Table III.

Expression (10), in conjunction with numerical values for ξ_i, can be used to generate model ESR spectra for K_3. In Fig. 3 we display four such representative patterns representing the expected high-field spectra for stable linear, obtuse, equilateral, and acute structures. Plotted also for reference are the resonance positions for K atoms. In the K_3 spectra, each line corresponds to a set of nuclear-spin configurations in the cluster; the heights are proportional to the degeneracy of the nuclear state with respect to

TABLE III. Structure dependence of nuclear-spin densities for K_3. Values for the parameters ξ_A and ξ_B, defined in the text, are given here for the structures described in Set II of Table II. The subscripts A and B refer to the apex (nonequivalent) atom and the base atoms, respectively. Some of these values are used in the generation of the model hyperfine spectra of Fig. 3.

θ_A	ξ_A (a.u.)$^{-3}$	ξ_B (a.u.)$^{-3}$
180	−0.125	0.357
90	−0.104	0.383
75	−0.101	0.405
60	0.338	0.338
55	0.885	0.148
50	1.02	0.050

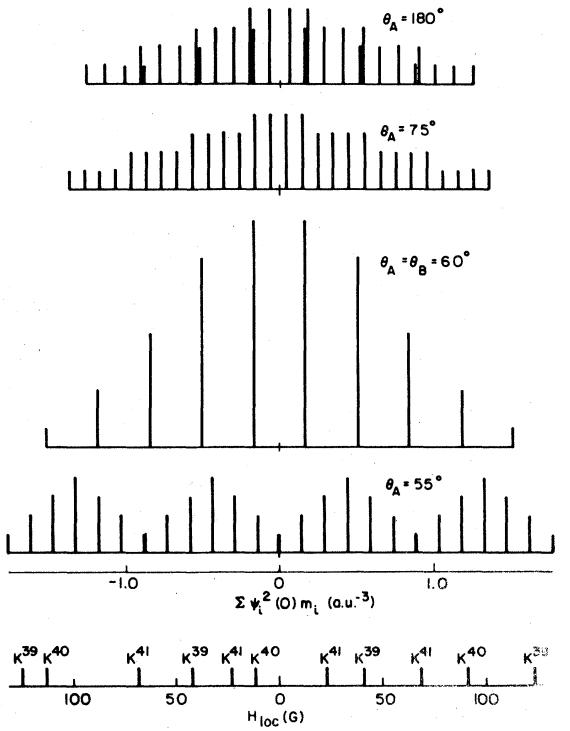

FIG. 3. Model hyperfine spectra K_3. The XASW calculations of ξ_i in Table III are used here to predict the appearance of the K_3 ESR spectra for several different geometries. θ_A is the included angle at the nonequivalent (apex) atom; θ_B is the included angle at the two base atoms.

$M = \sum m_{Ii}$, where the sum is over equivalent nuclei. The horizontal axis is the effective local field H_{loc} due to the nuclei, with $H_{\text{loc}} = 0$ at the free-electron transition field.

The division of the pattern for the obtuse and linear structures into seven groups of four lines each reflects the b_2 symmetry of the orbital occupied by the unpaired majority spin, which is characterized by a node at the apex nucleus. The splitting in each of the seven groups is thus a direct result of the core polarization of the remaining electrons of largely s character via their exchange interaction with the unpaired majority spin. The difference in sign of the spin densities for the apex and base atoms obtained here for the linear case are in agreement with the RHF + CI result of Kendrick[27] for linear Li_3, but we find this difference in sign occurring even for obtuse K_3 structures, in contrast to the corresponding calculations for Li_3. The four major features of the model spectrum of Fig. 3 for the acute configuration correspond to the possible orientations of the apex nucleus, at which we find considerable spin pile up, also consistent with Kendrick's result[27] for Li_3. The valence wave functions for the

acute case are all of a_1 character, so that the enhancement of the apex spin density is the result of the proximity of the two equivalent base atoms assumed for this calculation, rather than any nodal features imposed by symmetry on the valence spin orbitals. It is interesting to note in this connection that the most obtuse of the calculated structures exhibits nuclear-spin densities quite close to the dimer + atom limit, as is evident from the values of ξ in Table III. As the two base atoms approach each other, the net spin density at the nucleus approaches the dimer limit of $\xi_B = 0$, while for the apex atom, ξ_A approaches the value $\xi_{atom} = 1.11$ (a.u.)$^{-3}$ inferred from the zero-field splitting measurements of Kusch and Hughes[36] on K atoms.

Both the anisotropic hyperfine interaction $\mathcal{H}_{anis}$, and the contribution to the electron g value from spin-orbit coupling are estimated to be of little importance compared to the isotropic interaction of Eq. (6) in the determination of the appearance of the ESR spectrum of K_3. The interaction $\mathcal{H}_{anis}$ has the form

$$\mathcal{H}_{anis} = -\sum_i \frac{g\mu_0\mu_i}{I}\left(\frac{\vec{S}\cdot\vec{I}_i}{r_i^3} - \frac{3(\vec{S}\cdot\vec{r}_i)(\vec{I}_i\cdot\vec{r}_i)}{r_i^5}\right) \quad (11)$$

and appears as a broadening of the ESR spectral lines for a randomly oriented (powder) sample. The contribution arises from the non-s component of the electronic wave function with respect to the individual nuclei. For K_3 we estimate from our XASW wave functions that $\mathcal{H}_{anis}$ contributes a width corresponding to $(\Delta H_R)_{rms} \sim 3$ G to the line corresponding to maximum M, for which the effect is expected to be largest. Similarly, an estimate of the effect of spin-orbit $(\vec{L}\cdot\vec{S})$ coupling arising from admixture of non-s character into the orbitals predicts a g shift of $\Delta g_{zz}/g \sim 3\times 10^{-6}$.

IV. CONCLUSIONS

The model ESR spectra for K_3 given here are suitable for comparison with high-field measurements on this species in the determination of its molecular structure. The calculation is based on the assumptions of (1) a stabilized geometrical configuration for the trimer and (2) an interactionless environment. While assumption (1) may be justified for the matrix ESR measurements of Lindsay *et al.*,[2,3,37] their observed dependence of the atomic hyperfine coupling and g shift on the matrix trapping-site environment suggests that care should be taken in any direct quantitative comparison with theory. The study of such site interactions is, however, interesting in itself and is a natural extension of the current work.

The measured contact interaction for K atoms varies by about 6% from site to site,[3] and so a qualitative comparison with the current calculations is not precluded. Of the K_3 structures we have studied, the obtuse configurations yielded the spin densities in closest agreement with the matrix observations of Lindsay *et al.*[3] The core-polarization spin density for the apex nucleus inferred from their data is ~63% of our theoretical result for obtuse K_3, while our calculated contact spin density for the equivalent base atoms is only 77% of their measured value. These discrepancies could quite possibly reflect our assumed bond lengths.

In contrast to the situation for low-temperature matrix measurements, molecular-beam measurements may afford a good basis for comparison with the above model spectra if, in fact, the internal temperature of the aggregate can be lowered sufficiently so that a stabilized configuration can be observed. While the work of Gerber and Schumacher[25] on Li_3 strongly suggests that this last requirement cannot be met in this species due to the flatness of its energy hypersurface compared to the zero-point vibrational energies, calculations such as those of Martin and Davidson[24] for Na_3, on the other hand, indicate that stabilized configurations may in fact exist for the heavier alkali trimers, making possible the comparison of ESR measurements with model spectra such as those of Fig. 3.

ACKNOWLEDGMENTS

It is my pleasure to acknowledge Professor D. A. Case for his generous gift of the XASW routine and for stimulating discussions with regard to the current work. I also thank Professor W. D. Knight, who has given me a great deal of support and encouragement and who, along with Alan George, participated in many stimulating discussions of this interesting problem. This work was supported in part by the Division of Materials Research, National Science Foundation, and is in partial fulfillment of the requirements for the Ph.D. degree.

*Present address: Department of Physics, University of Hawaii, Honolulu, Hawaii 96822.

[1] J. C. Slater and K. H. Johnson, Phys. Today 27, 34 (1974).

[2] D. M. Lindsay, D. R. Herschbach, and A. L. Kwiram, Mol. Phys. 32, 1199 (1976).

[3] D. M. Lindsay, and G. A. Thompson, Bull. Am. Phys. Soc. 25, 244A (1980).

[4]E. J. Robbins, R. E. Leckenby, and P. Willis, Adv. Phys. 16, 739 (1967).
[5]P. J. Foster, R. E. Leckenby, and E. J. Robbins, J. Phys. B 2, 478 (1969).
[6]A. Hermann, E. Schumacher, and L. Wöste, J. Chem. Phys. 68, 2327 (1978).
[7]A. Hermann, S. Leutwyler, E. Schumacher, and L. L. Wöste, Helv. Chim. Acta 61, 453 (1978).
[8]A. Hermann, S. Leutwyler, E. Schumacher, and L. Wöste, Chem. Phys. Lett. 52, 418 (1977).
[9]A. Hermann, M. Hofmann, S. Leutwyler, E. Schumacher, and L. Wöste, Chem. Phys. Lett. 62, 216 (1979).
[10]A. Herman, S. Leutwyler, L. Wöste, and E. Schumacher, Chem. Phys. Lett. 62, 444 (1979).
[11]E. R. Dietz, Ph.D. thesis, University of California, Berkeley, 1980 (unpublished).
[12]W. D. Knight, E. R. Dietz, A. R. George, and W. H. DeHeer (unpublished).
[13]A. L. Companion, D. J. Steible, and A. J. Starshak, J. Chem. Phys. 49, 3637 (1968).
[14]B. T. Pickup, Proc. R. Soc. London Ser. A 333, 69 (1973).
[15]B. T. Pickup and W. Byers-Brown, Mol. Phys. 23, 1189 (1972).
[16]J. C. Whitehead and R. Grice, Mol. Phys. 26, 267 (1973).
[17]A. Gelb, K. D. Jordon, and R. Silbey, Chem. Phys. 9, 175 (1975).
[18]J. G. Fripiat, K. T. Chow, M. Boudart, J. R. Diamond, and K. H. Johnson, J. Mol. Catalysis 1, 59 (1975).
[19]R. C. Baetzold and R. E. Mack, Inorg. Chem. 14, 686 (1975).
[20]G. A. Hart and P. L. Goodfriend, Mol. Phys. 29, 1109 (1975).
[21]D. W. Davies and G. Del Conde, Discuss. Faraday Soc. 55, 369 (1973); Chem. Phys. 12, 45 (1976).
[22]D. W. Davies and G. Del Conde, Mol. Phys. 33, 1813 (1977).
[23]J. Kendrick and I. H. Hillier, Mol. Phys. 33, 635 (1977).
[24]R. L. Martin and E. R. Davidson, Mol. Phys. 35, 1713 (1978). See Table 5 and the discussion immediately following for values of average bond lengths and energies for the Na dimer, trimer, and bulk.
[25]W. H. Gerber and E. Schumacher, J. Chem. Phys. 69, 1692 (1978).
[26]A. L. Companion, Chem. Phys. Lett. 56, 500 (1978).
[27]J. Kendrick, Mol. Phys. 35, 593 (1978).
[28]J. C. Slater in *Advances in Quantum Chemistry*, edited by P.-O. Lowdin (Academic, New York, 1972), Vol. 6, pp. 1–92.
[29]K. H. Johnson in *Advances in Quantum Chemistry*, edited by P.-O. Lowdin (Academic, New York, 1973), Vol. 7, pp. 143–185.
[30]K. Schwarz, Phys. Rev. B 5, 2466 (1972).
[31]J. B. Mann, Los Alamos Scientific Laboratory Report No. LA-3690, 1967 (unpublished).
[32]D. R. Salahub, R. P. Messmer, and K. H. Johnson, Mol. Phys. 31, 529 (1976).
[33]See, for example, J. C. Slater, *The Calculation of Molecular Orbitals* (Wiley, New York, 1979).
[34]G. Herzberg, *Diatomic Molecules* (Prentice-Hall, New York, 1966).
[35]The terms acute and obtuse here refer to apex angles less than and greater than 60°, respectively.
[36]P. Kusch and V. W. Hughes, in *Handbuch der Physik*, edited by S. Flügge (Springer, Berlin, 1959).
[37]D. M. Lindsay, D. R. Hershbach, and A. L. Kwiram, Mol. Phys. 39, 529 (1980).